

Molecular gas dynamics observations of Chapman-Enskog behavior and departures therefrom in nonequilibrium gases

M. A. Gallis, J. R. Torczynski, and D. J. Rader

Engineering Sciences Center, Sandia National Laboratories, Albuquerque, New Mexico 87185, USA

(Received 15 April 2003; revised manuscript received 22 August 2003; published 29 April 2004)

Bird's direct simulation Monte Carlo method is used to compute the molecular velocity distribution of a gas with heat flow. At continuum nonequilibrium conditions (small heat flux), Chapman-Enskog behavior is obtained for inverse-power-law molecules (hard-sphere through Maxwell): the Sonine-polynomial coefficients away from walls (i.e., the normal solution) agree with theory. At noncontinuum nonequilibrium conditions (large heat flux), these coefficients differ systematically from their continuum values as the local Knudsen number (nondimensional heat flux) is increased.

DOI: 10.1103/PhysRevE.69.042201

PACS number(s): 51.10.+y, 02.70.Ns, 05.20.Dd, 47.45.-n

A dilute monatomic gas is described by the Boltzmann equation (BE) [1]. Chapman-Enskog (CE) theory solves the BE as a series expansion in powers of the local Knudsen number Kn [2]. The first-order terms yield the (equilibrium) Maxwellian velocity distribution: $f^{(0)} = (\sqrt{\pi}c_m)^{-3} \exp[-c^2/c_m^2]$, where \mathbf{c} is the thermal velocity, $c_m = (2k_B T/m)^{1/2}$ is the most probable thermal speed, m is the molecular mass, T is the temperature, and $k_B = 1.380658 \times 10^{-23}$ J/K is the Boltzmann constant. The second-order terms yield the (continuum) CE velocity distribution: $f = f^{(0)}\{1 + \Phi^{(1)}\}$. The higher-order terms are significant for noncontinuum conditions (i.e., when Kn is not small), but this situation is not well understood. The goal here is to determine the normal-solution velocity distribution (i.e., outside the Knudsen layers at solid surfaces) during heat flow when Kn is not small and (second-order) CE theory is not accurate.

Molecular gas dynamics can simulate continuum and non-continuum nonequilibrium gas conditions: no assumption is made regarding the magnitude of Kn . This approach is embodied in the direct simulation Monte Carlo (DSMC) method of Bird [1]. Arguments that DSMC solves the BE were advanced originally by Bird [3]. Recently, Wagner [4] presented a formal mathematical proof that has been accepted as valid [5].

In DSMC, large numbers of computational molecules represent the gas. During a time step, these molecules move ballistically, reflect from boundaries (diffuse, specular, etc.), and collide with other molecules in the same computational cell. Time steps are small compared to the mean collision time, and cells are small compared to the mean free path. Because the gas is dilute, only binary collisions are allowed, and these collisions are performed stochastically (molecular chaos). The collision rate is determined by the number density and the thermal-energy density of molecules in a cell. The post-collision velocities reproduce the angular distribution of the prescribed molecular interaction. For steady conditions, the velocity distribution is determined by sampling molecules over long times.

The variable soft sphere (VSS) method is used to select post-collision velocities [1]. The collision process is specified in terms of a reference molecular "diameter" [1]:

$$d_{\text{ref}} = \left(\frac{5(\alpha+1)(\alpha+2)(mk_B T_{\text{ref}}/\pi)^{1/2}}{4\alpha(5-2\omega)(7-2\omega)\mu_{\text{ref}}(\mu_1/\mu_\infty)} \right)^{1/2}, \quad (1)$$

where μ_{ref} is the viscosity at a reference temperature T_{ref} and ω and α describe collision dynamics. This prescription leads to a thermal conductivity at T_{ref} of $K_{\text{ref}} = (K_\infty/K_1)(15/4)(k_B/m)\mu_{\text{ref}}(\mu_1/\mu_\infty)$.

The quantities μ_∞/μ_1 and K_∞/K_1 are CE ratios of the infinite-approximation to first-approximation values of viscosity and thermal conductivity, respectively [2]. These quantities are obtained for VSS molecules from the equivalent "inverse-power-law" (IPL) molecules, point centers of a repulsive force that varies with the intermolecular separation r according to $1/r^\nu$. The viscosity and thermal conductivity of IPL and VSS molecules have a temperature dependence of T^ω , where $\omega = (1/2) + [2/(\nu-1)]$ [2]. Molecules with $\omega = 1/2$ ($\nu = \infty$) have a hard-sphere interaction, whereas molecules with $\omega = 1$ ($\nu = 5$) have a Maxwell interaction. Real molecules generally have ω values between these extremes [1,2]. As in Table I, the quantities μ_∞/μ_1 , K_∞/K_1 , and D_∞/D_1 (self-diffusion coefficient) are close to unity for IPL molecules with $1/2 \leq \omega \leq 1$ [6]. For a VSS molecule with ω , the parameter α is found by equating the VSS and IPL Schmidt numbers [1]: $\alpha = 2A_2[\nu]/(2A_1[\nu] - A_2[\nu])$, where the functions $A_1[\nu]$ and $A_2[\nu]$ are given by Chapman and Cowling [2].

TABLE I. Chapman-Enskog results.

| Quantity | Hard-sphere | Maxwell |
|--------------------|-------------|---------|
| ω | 1/2 | 1 |
| α | 1 | 2.13986 |
| μ_∞/μ_1 | 1.016034 | 1 |
| K_∞/K_1 | 1.025218 | 1 |
| D_∞/D_1 | 1.018954 | 1 |
| a_1/a_1 | 1 | 1 |
| a_2/a_1 | 0.0954284 | 0 |
| a_3/a_1 | 0.0217503 | 0 |
| a_4/a_1 | 0.0068579 | 0 |
| a_5/a_1 | 0.0025926 | 0 |

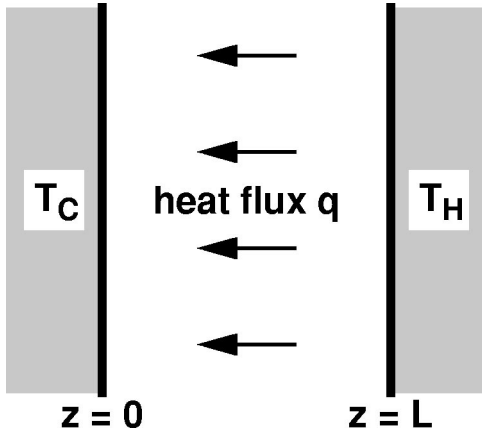


FIG. 1. Schematic diagram of domain.

A motionless gas transporting heat is considered (see Fig. 1). Gas molecules are confined between two infinite parallel walls at unequal temperatures, from which molecules reflect diffusely with complete accommodation. This situation is mathematically one dimensional. The walls are placed many mean free paths apart so that the Knudsen layers occupy small portions of the domain near the walls and the normal solution occupies the central region.

The CE distribution for continuum conditions is expressed as a sum of Sonine polynomials [2]:

$$\Phi^{(1)} = -(8/5)(K/K_{\text{eff}})\tilde{A}[\tilde{c}]\tilde{c}\cdot\tilde{q}, \quad (2)$$

$$\tilde{A}[\tilde{c}] = \sum_{k=1}^{\infty} (a_k/a_1)S_{3/2}^{(k)}[\tilde{c}^2], \quad (3)$$

$$S_j^{(k)}[x] = \sum_{i=0}^k \frac{(j+k)!(-x)^i}{(j+i)!i!(k-i)!}, \quad (4)$$

where $K = -(5/4)k_B c_m^2 a_1$ is the thermal conductivity, q is the heat flux, $q \equiv K_{\text{eff}} |\partial T / \partial z|$ defines the effective thermal conductivity, $\tilde{q} = q / (m n c_m^3)$ is the nondimensional heat flux, $\tilde{c} = c / c_m$ is the nondimensional thermal velocity, and $\text{Kn} \equiv \tilde{q}$ defines the local Knudsen number. Although $K/K_{\text{eff}} = 1$ in the CE distribution, this may not be true in general. For the geometry above, it has been proved that $K/K_{\text{eff}} = 1$ at arbitrary heat fluxes for Maxwell and BGK interactions [7,8], and computations have suggested this for the hard-sphere interaction [9]. The coefficients a_k of the Sonine polynomials $S_{3/2}^{(k)}$ depend on the type of interaction. CE theory [2] can be used to determine infinite-approximation values for the a_k , and hence the a_k/a_1 , for IPL molecules (see Table I). The quantities K/K_{eff} and a_k/a_1 can also be determined from DSMC simulations. CE theory relates K/K_{eff} to computed or known quantities:

$$\frac{K}{K_{\text{eff}}} = \left(\frac{K_{\infty}}{K_1} \right) \left(\frac{\mu_1}{\mu_{\infty}} \right) \left(\frac{15}{4} \right) \left(\frac{k_B}{m} \right) \left(\frac{\mu_{\text{ref}}}{T_{\text{ref}}} \right) \left(\frac{T^{\omega}}{q} \right) \left(\frac{\partial T}{\partial z} \right). \quad (5)$$

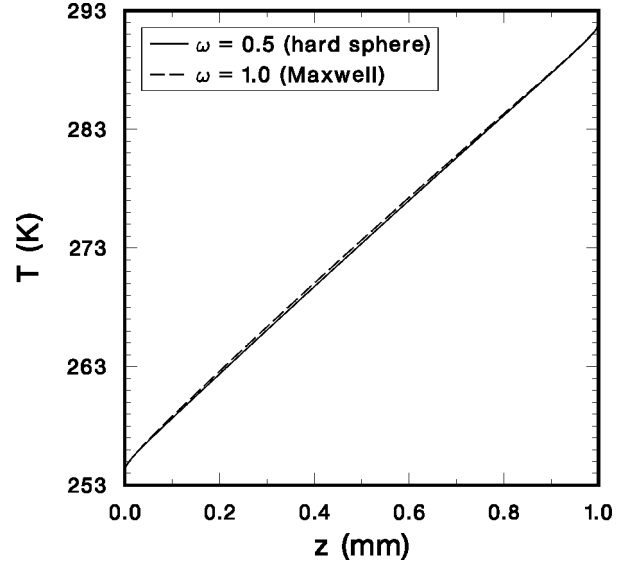


FIG. 2. Temperature profiles for continuum conditions.

The first five factors are known constants, and T , q , and $\partial T / \partial z$ are computed. The a_k/a_1 involve moments of powers of thermal velocity components, where $\langle \tilde{c}^{2i} \tilde{c}_z \rangle = \langle c^{2i} c_z \rangle / c_m^{2i+1}$:

$$\frac{a_k}{a_1} = \left(\frac{15\sqrt{\pi}}{8} \right) \sum_{i=1}^k \left(\frac{(-1)^{i-1} k!}{i!(k-i)! \left(i + \frac{3}{2} \right)!} \right) \left(\frac{\langle \tilde{c}^{2i} \tilde{c}_z \rangle}{\langle \tilde{c}^2 \tilde{c}_z \rangle} \right). \quad (6)$$

DSMC simulations are performed for the situation in Fig. 1. Argon properties are used [1,6]: $m = 66.3 \times 10^{-27}$ kg and $\mu_{\text{ref}} = 2.117 \times 10^{-5}$ Pa s at $T_{\text{ref}} = 273.15$ K. The cold wall at $z=0$ has $T_C = T_{\text{ref}} - \Delta T/2$, and the hot wall at $z=L$ has $T_H = T_{\text{ref}} + \Delta T/2$. Here, $L = 1$ mm. The number density n corresponds to a pressure of $p = 133.3$ or 266.6 Pa at T_{ref} . The mean free path $\lambda = \sqrt{\pi} \mu / m n c_m$ is 0.0237 mm at 266.6 Pa and 273.15 K, so $L \approx 42\lambda$ at these conditions. Temperature differences ΔT of 20, 40, 100, 200, 300, and 400 K are used.

Simulations are performed using Bird's DSMC1 code [1], as modified to sample both precollision and postcollision molecules. Uniform cell sizes Δz of 10, 5, and $2.5 \mu\text{m}$ (i.e., 100, 200, and 400 cells) are used with time steps Δt of 14, 7, and 3.5 ns, respectively, and 30–60 molecules per cell are used, all of which satisfy Bird's accuracy criteria [1]. Results for different meshes, time steps, and numbers of molecules exhibit the expected convergence behavior [10–12]. The results below are obtained using the $2.5\text{-}\mu\text{m}$ cell size and the 3.5-ns time step with 30 molecules per cell, for which the heat flux is estimated to have an uncertainty of 0.2%. Simulations are initialized with spatially uniform properties at the reference conditions, and the transient flow is allowed to decay for 2.1 ms, far longer than needed to achieve steady state. Statistics are collected for $O(10^9)$ time steps, so $O(10^{10})$ molecules are sampled per cell. Each simulation is run for 60–120 h on 16–32 nodes of an IBM Linux cluster, where each node has dual 1.2-GHz P3 processors.

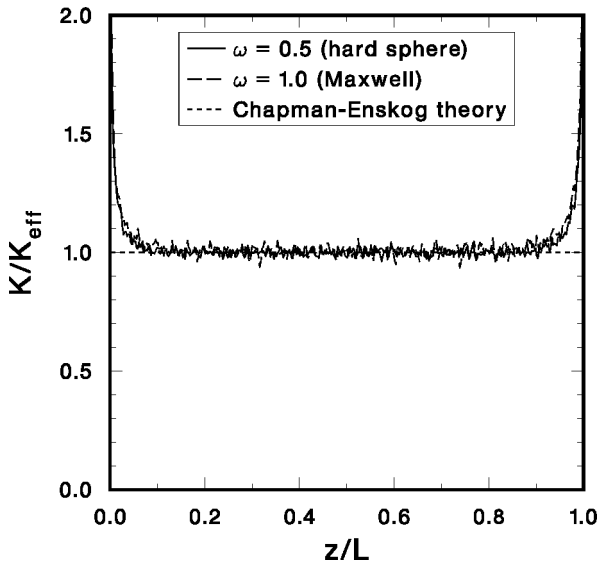


FIG. 3. Conductivity-ratio profiles for continuum conditions.

Simulation results for hard-sphere and Maxwell interactions at $p=266.6$ Pa and $\Delta T=40$ K are shown in Figs. 2–4. The temperature profiles in Fig. 2 exhibit small jumps near the walls and a nearly linear profile in the central region [6]. The statistical variations are too small to be observed because of the large number of molecules sampled per cell. The conductivity-ratio profiles in Fig. 3 obtain the theoretical value of $K/K_{\text{eff}}=1$ to within the uncertainty in the central region, where the normal solution is obtained. The Knudsen layers are easily seen in these profiles as departures from unity. The statistical variations in these profiles are larger because the temperature gradient is determined by central differences.

Figure 4 shows profiles of the Sonine-polynomial coefficients a_k/a_1 for $k=2, 3, 4, 5$ along with CE values for the hard-sphere interaction. Excellent agreement is seen in the

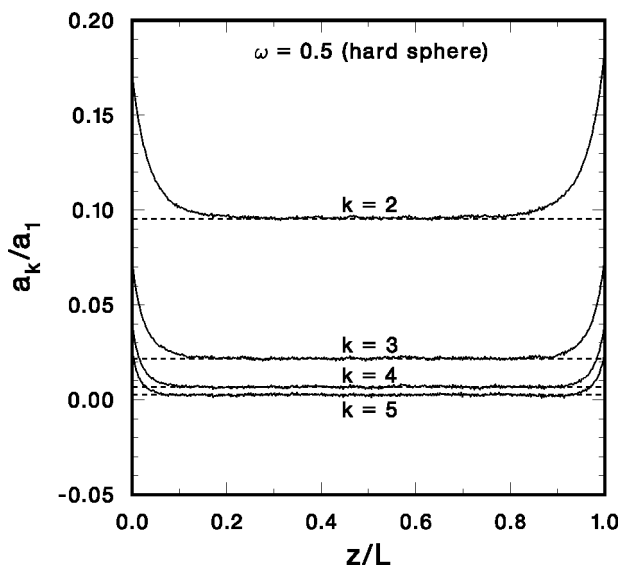


FIG. 4. Solid curves, coefficient profiles for continuum conditions; dashed lines, CE values.

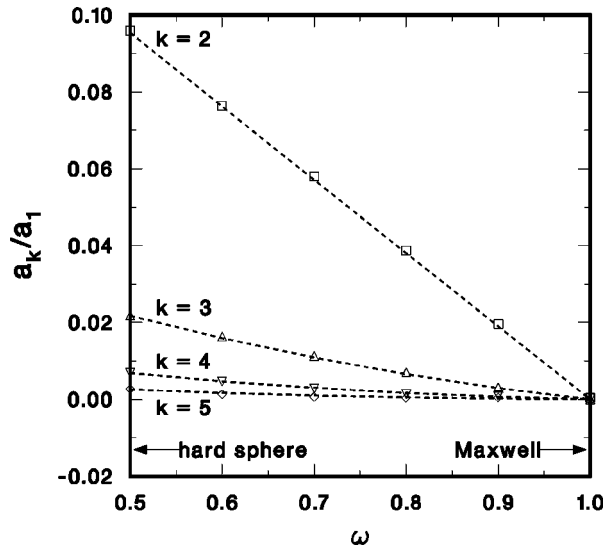


FIG. 5. Effect of molecular interaction: symbols, coefficients for continuum conditions; dashed curves, CE values.

central region, where the normal solution is obtained. Although not shown, the a_k/a_1 for $k=6, 7, 8, 9$ exhibit similarly good agreement. Simulation results for $p=133.3$ Pa and/or $\Delta T=20$ K are essentially the same except that the profiles have thicker Knudsen layers at the lower pressure and more statistical variation at the lower temperature difference.

Simulation results for $1/2 \leq \omega \leq 1$ at $p=266.6$ Pa and $\Delta T=40$ K are compared with CE theory in Fig. 5. The symbols are the simulation values of a_k/a_1 for $k=2, 3, 4, 5$ averaged over the central 40% of the domain (i.e., the normal solution), and the curves are the CE values. Agreement is good over the entire range of ω .

Figure 6 shows simulation results for the hard-sphere interaction at $p=266.6$ Pa and $\Delta T=200$ K. Since the local

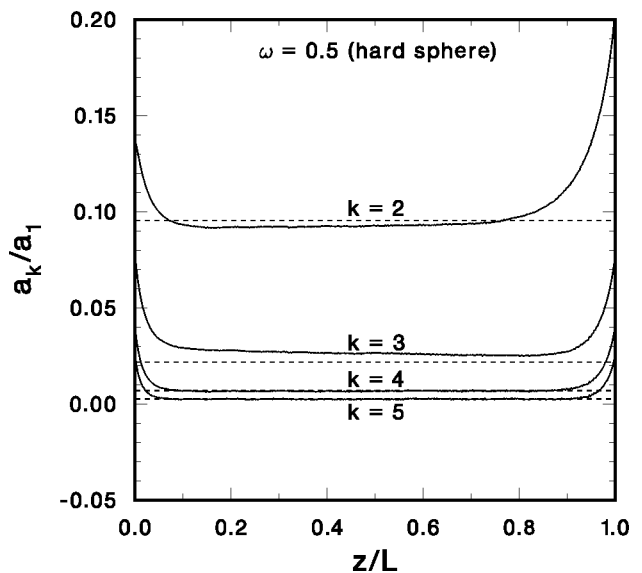


FIG. 6. Solid curves, coefficient profiles for noncontinuum conditions; dashed lines, CE values.

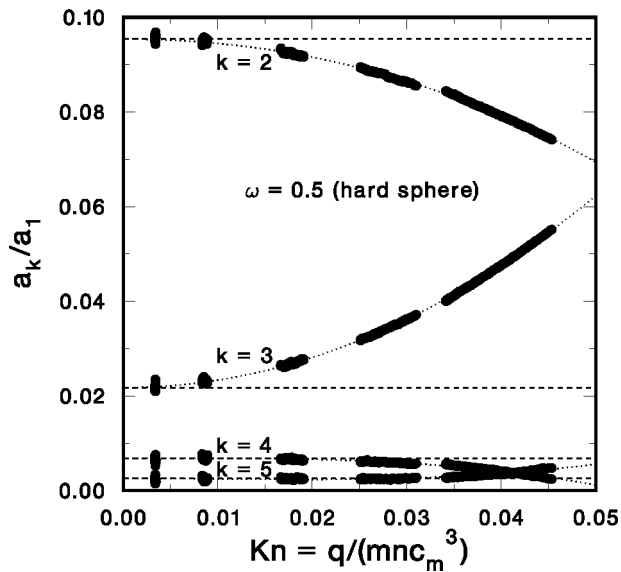


FIG. 7. Symbols linked by dotted curves, coefficients vs local Knudsen number (nondimensional heat flux); dashed lines, CE values.

Knudsen number $Kn \equiv q/(mnc_m^3) = O(0.02)$ for this case, the conditions are noncontinuum, so CE theory does not accurately represent the gas: the Sonine-polynomial coefficients depart from the CE values in the central region. The profiles are closer to the CE values on the hot side of the central region because conditions there are more “continuum:” Kn is smaller because the heat flux q is constant throughout the domain, the pressure $p = (mnc_m^2)/2$ (the ideal gas law) is approximately constant, and the most probable speed c_m is larger on the hot side. Although not shown, the same degree of difference between simulation results and CE theory is observed for the Maxwell interaction at these conditions.

Figure 7 shows simulation results quantifying the dependence of the normal-solution Sonine-polynomial coefficients on Kn for the hard-sphere interaction. Each cluster of points corresponds to a single temperature difference, and each point within a cluster corresponds to a location within $5/16 \leq z/L \leq 9/16$. For $Kn = O(0.05)$, the molecular velocity distribution differs significantly from the CE distribution a_3/a_1 is comparable to a_2/a_1 , and a_5/a_1 exceeds a_4/a_1 . The trend that even-index coefficient ratios decrease and odd-index coefficient ratios increase with increasing Kn is also observed for the Maxwell interaction.

The conductivity-ratio profiles for both molecular interactions at all temperature differences are similar to Fig. 3: the CE value of 1 is achieved in the central region. Additionally, the pressure portion of the stress tensor remains isotropic for the Maxwell interaction but becomes increasingly anisotropic for the hard-sphere interaction as Kn is increased. These facts agree with previous theoretical and computational results [7–9] and provide strong evidence that the simulation results are accurate and that the normal solution is achieved in the central region.

Molecular gas dynamics is a viable approach for investigating nonequilibrium gases. The DSMC method accurately reproduces the subtle effects of molecular interaction on the CE velocity distribution function (i.e., the normal solution). Excellent agreement is obtained between DSMC and CE theory for a stationary gas with a small heat flux (continuum conditions), whereas significant differences are observed and quantified at large heat fluxes (noncontinuum conditions).

This work was performed at Sandia National Laboratories. Sandia is a multiprogram laboratory operated by Sandia Corporation, a Lockheed Martin Company, for the United States Department of Energy under contract DE-AC04-94AL85000. The authors thank Professor A. Santos of the Universidad de Extremadura for helpful discussions.

-
- [1] G. A. Bird, *Molecular Gas Dynamics and the Direct Simulation of Gas Flows* (Clarendon Press, Oxford, 1998).
- [2] S. Chapman and T. G. Cowling, *The Mathematical Theory of Non-Uniform Gases* (Cambridge University Press, Cambridge, 1970).
- [3] G. A. Bird, *Phys. Fluids* **13**, 2676 (1970).
- [4] W. Wagner, *J. Stat. Phys.* **66**, 1011 (1992).
- [5] C. Cercignani, *Rarefied Gas Dynamics: From Basic Concepts to Actual Calculations* (Cambridge University Press, Cambridge, 2000).
- [6] M. A. Gallis, D. J. Rader, and J. R. Torczynski, *Phys. Fluids* **14**, 4290 (2002).
- [7] E. S. Asmolov, N. K. Makashev, and V. I. Nosik, *Sov. Phys. Dokl.* **24**, 892 (1979).
- [8] A. Santos, J. J. Brey, and V. Garzo, *Phys. Rev. A* **34**, 5047 (1986).
- [9] J. M. Montanero, M. Alaoui, A. Santos, and V. Garzo, *Phys. Rev. E* **49**, 367 (1994).
- [10] F. J. Alexander, A. L. Garcia, and B. J. Alder, *Phys. Fluids* **10**, 1540 (1998).
- [11] A. L. Garcia and W. Wagner, *Phys. Fluids* **12**, 2621 (2000).
- [12] N. G. Hadjiconstantinou, *Phys. Fluids* **12**, 2634 (2000).